Supporting Information for

Chitosan-based asymmetric topological membranes with cell-like features for healthcare applications

Yulin Jiang,[‡a] Yi Deng,[‡ac] Ying Tu,[a] Birol Ayb,[d] Xiaodong Sun,[a] Yubao Li,[a] Xiaohong Wang,[b] Xianchun Chen*[a] and Li Zhang*[a]

[a] Analytical and Testing Center, Research Center for Nano-biomaterials, & School of Chemical Engineering, & West China School of Preclinical and Forensic Medicine, & School of Materials Science & Engineering, Sichuan University, Chengdu 610065,

[b] State Key Laboratory of Marine Resource Utilization in South China Sea, Hainan University, Haikou 570228, China

[c] Department of Mechanical Engineering, The University of Hong Kong, Hong Kong SAR, China

[d] Institute of Biomaterials and Biomedical Engineering, University of Toronto, Toronto, Ontario M5S 3E3, Canada

*Corresponding author

Prof. Li Zhang: nic1976@scu.edu.cn; zhangli9111@126.com

‡Yulin Jiang and Yi Deng contributed equally to this work.

Supplementary Figure Captions

Fig. S1 SEM images of nanoporous AAO templates after etching in the phosphoric acid solution for various etching times: (a) 0 min, (b) 25 min, (c) 50 min, and (d) 75 min.

Fig. S2 SEM images of the AAO nanotubes at different second oxidation times from top and cross-sectional views: (a) 60 min, (b) 90 min, and (c) 120 min.

Fig. S3 Scheme of cross-linking mechanism between STPP and chitosan.

Fig. S4 SEM images of the asymmetric EVA membranes with dense and spongy layers.

Fig. S5 The cross-linking degree of ATCS-4 and ATCS-8 membranes calculated by dissolving chitosan in chloroform (*$p < 0.05$, n = 6).

Fig. S6 SEM overview with low magnification of MG-63 culture on (a) SyCS, (b) ATCS-0, (c) ATCS-4, and (d) ATCS-8 membranes for 5 days.

Table S1. The pore size and surface porosity of the chitosan membranes.

Table S2. Tensile strength of the symmetric and asymmetric chitosan membranes under dry and wet conditions.

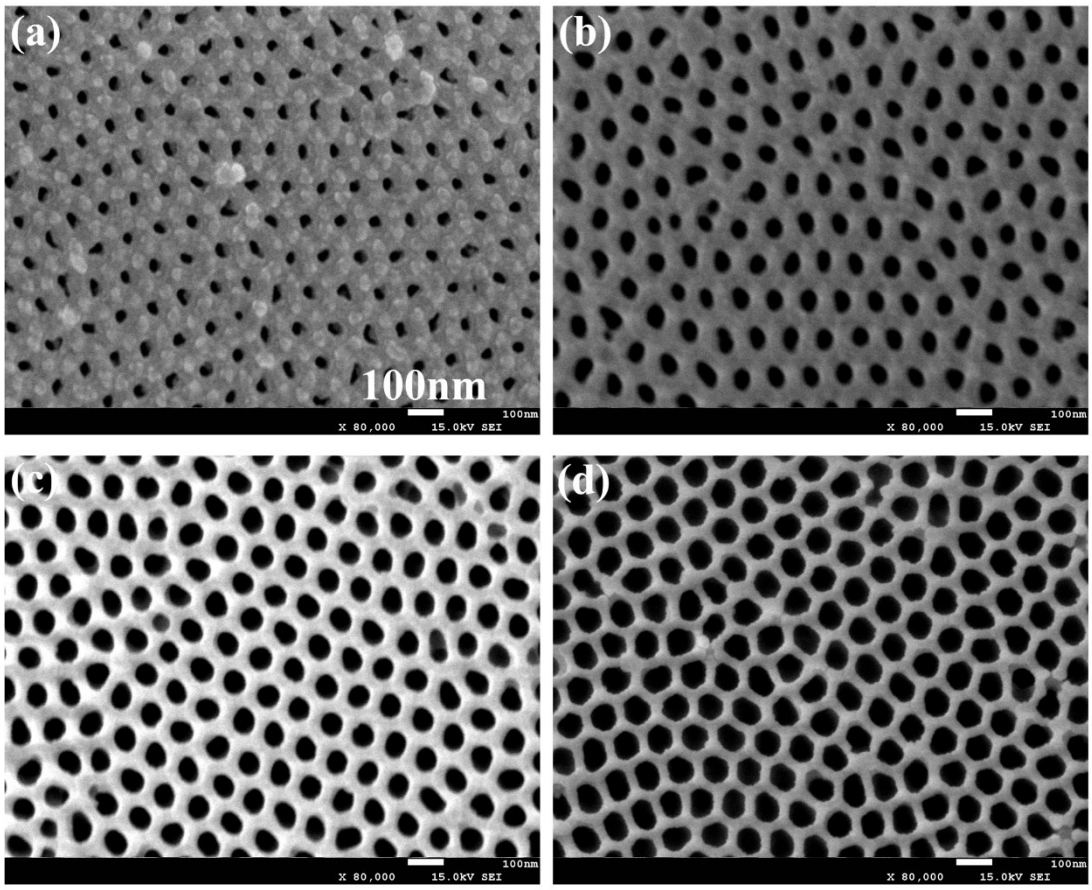

Fig. S1 SEM images of nanoporous AAO templates after etching in the phosphoric acid solution for various etching times: (a) 0 min, (b) 25 min, (c) 50 min, and (d) 75 min.

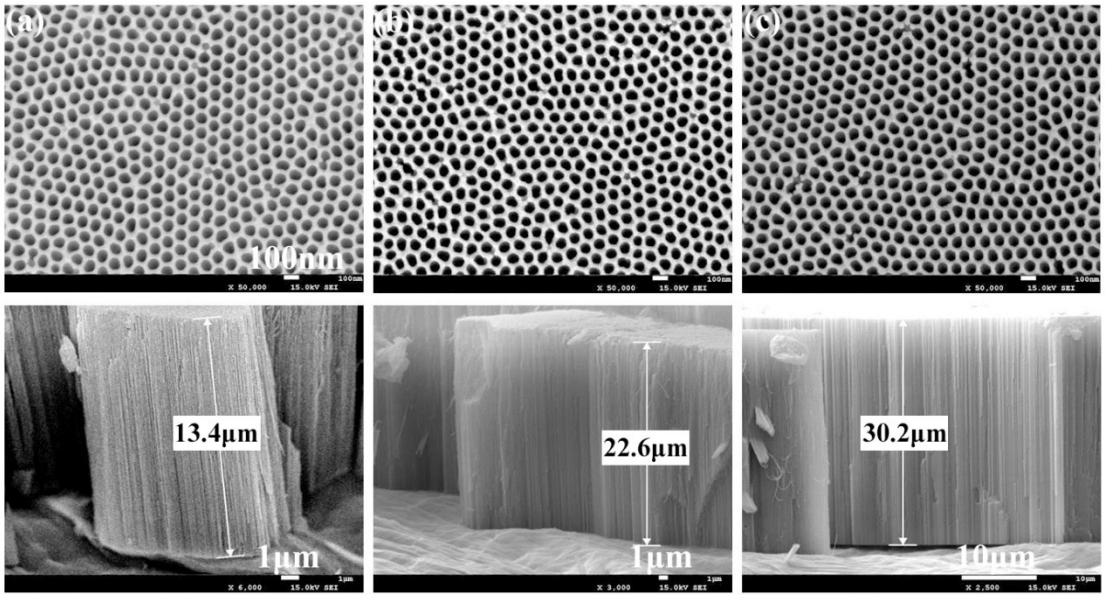

Fig. S2 SEM images of the AAO nanotubes at different second oxidation times from top and cross-sectional views: (a) 60 min, (b) 90 min, and (c) 120 min.

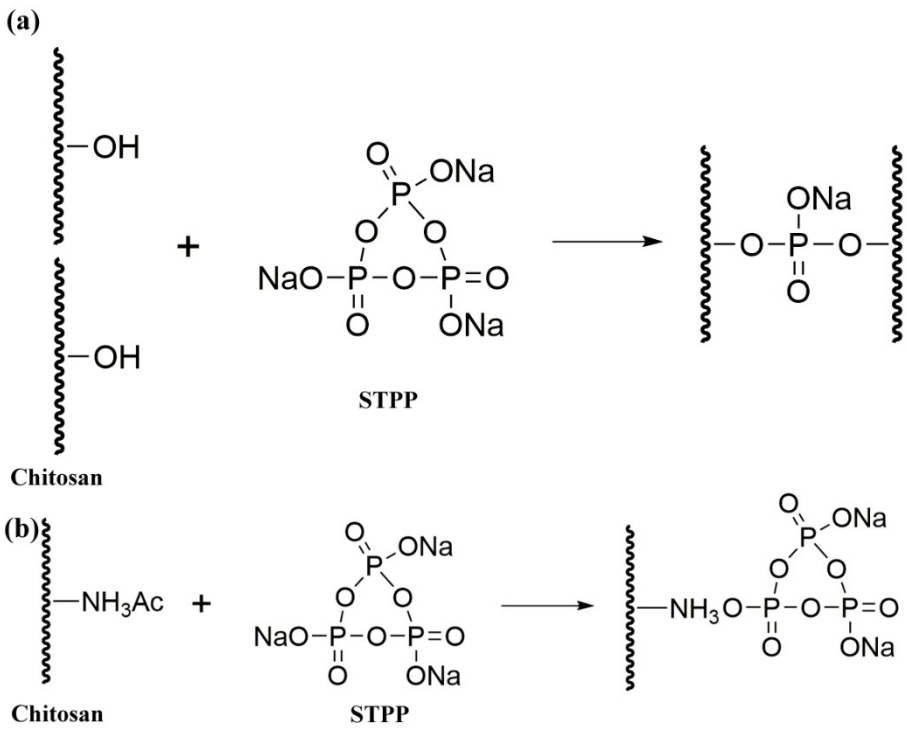

Fig. S3 Scheme of cross-linking mechanism between STPP and chitosan.

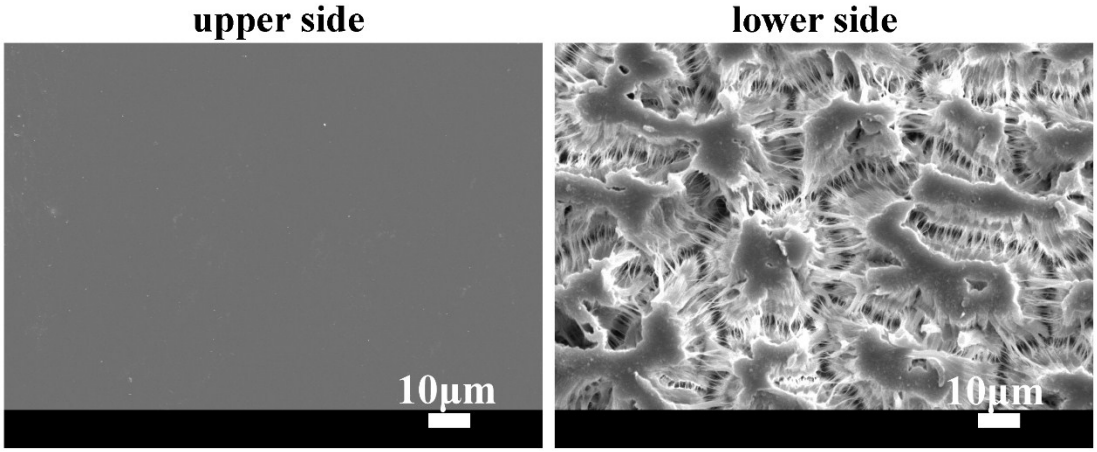

Fig. S4 SEM images of the asymmetric EVA membranes with dense and spongy layers.

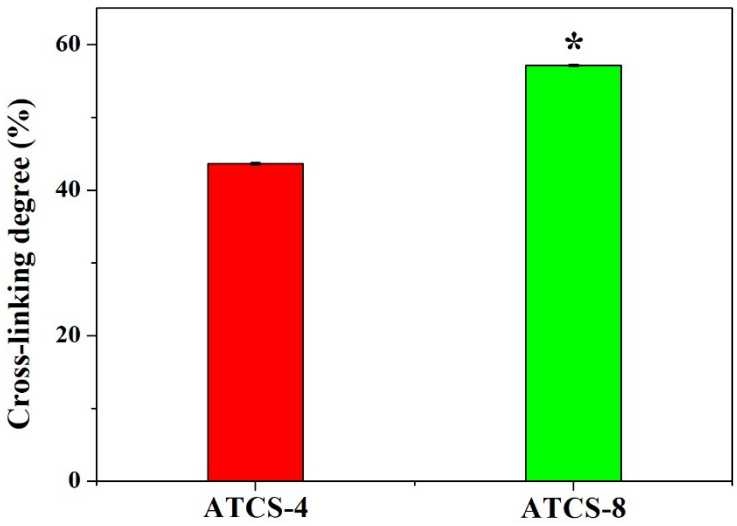

Fig. S5 The cross-linking degree of ATCS-4 and ATCS-8 membranes calculated by dissolving chitosan in chloroform (*$p < 0.05$, n = 6).

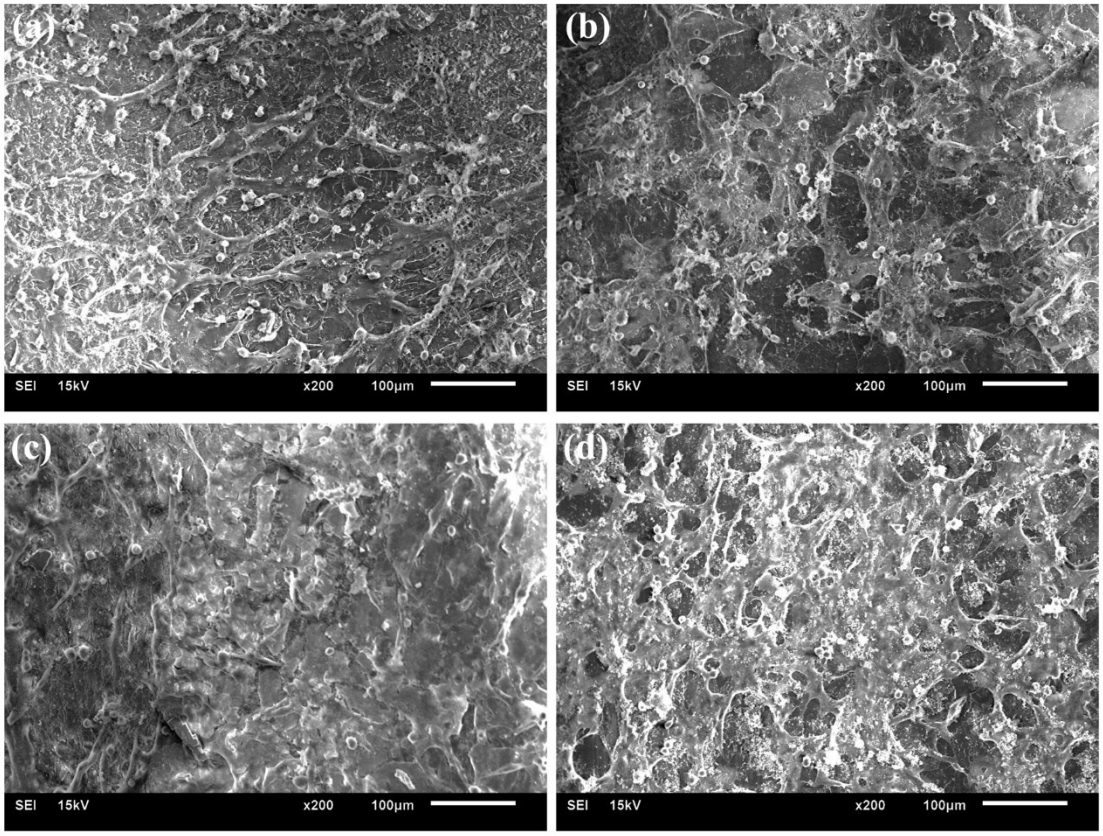

Fig. S6 SEM overview with low magnification of MG-63 culture on (a) SyCS, (b) ATCS-0, (c) ATCS-4, and (d) ATCS-8 membranes for 5 days.

Table S1. The pore size and surface porosity of the chitosan membranes.

Samples	Pore size (μm)	Surface porosity (%)
SyCS	0	0
ATCS-0	1.16 ± 0.01	13.04 ± 0.10
ATCS-4	1.08 ± 0.05	18.05 ± 0.43
ATCS-8	1.51 ± 0.03	22.56 ± 0.49

Table S2. Tensile strength of the symmetric and asymmetric chitosan membranes under dry and wet conditions.

Samples	Tensile strength in dry condition (MPa)	Tensile strength in wet condition (MPa)
SyCS	28.99 ± 2.35	3.74 ± 1.02
ATCS-0	19.36 ± 5.62	1.68 ± 0.34
ATCS-4	26.73 ± 1.15	3.45 ± 0.98
ATCS-8	30.32 ± 2.49	5.07 ± 1.10